Dhaka Univ. J. Biol. Sci. **34**(1): 1-23, 2025 (January) DOI: https://doi.org/10.3329/dujbs.v34i1.79834

DECIPHERING THE ANTICANCER POTENTIAL OF *LANNEA COROMANDELICA* TARGETING APOPTOSIS SIGNAL-REGULATORY KINASE 1 VIA ADVANCED COMPUTATIONAL BIOLOGY APPROACHES

Sheikh Sunzid Ahmed And M. Oliur Rahman*

Department of Botany, Faculty of Biological Sciences, University of Dhaka, Dhaka 1000, Bangladesh

Keywords: ASK1, *Lannea coromandelica*, molecular docking, molecular dynamics simulation, phytochemicals

Abstract

Colorectal cancer (CRC) is one of the leading causes of cancer-related mortality globally. The rising expenses, significant side effects, and increasing resistance to traditional CRC treatments suggest the critical need for new and more effective therapeutic options. This study explored the anticancer potential of *Lannea coromandelica* (Houtt.) Merr. phytocompounds targeting the promising apoptosis signal-regulatory kinase 1 (ASK1) protein using computational biology approaches including molecular docking, ADMET analysis, molecular dynamics (MD) simulation, and MM/GBSA calculations. Virtual screening of the 17 phytoconstituents identified two lead compounds: ellagic acid and physcion, with binding affinities of -9.6 kcal/mol and -9.3 kcal/mol, respectively. ADMET analysis revealed favorable pharmacokinetic, pharmacodynamic, and toxicity profiles for the lead compounds. MD simulations supported the stability and compactness of the two leads in comparison to the control drug erbitux for 200 ns. The lead compounds displayed fewer rotatable bonds compared to Erbitux, resulting in lower torsional flexibility and greater stability during the simulations. PCA-based essential dynamics analysis demonstrated highly similar global motions in phase space for both lead compounds and erbitux, indicating comparable dynamic properties. Free binding energy calculations identified ellagic acid (-69.20 kcal/mol) as the superior lead compound over physcion (-65.68 kcal/mol). These results may open new avenues for the development of novel drug candidates targeting colorectal cancer.

Introduction

Colorectal cancer (CRC) is the third most common cancer globally, making up about 10% of all cancer cases and ranking as the second leading cause of cancer-related deaths[(1)]. In 2020, over 1.9 million new cases and more than 935,000 deaths were linked to CRC

* Author for Correspondence: oliur.bot@du.ac.bd

worldwide, with notable regional variations in both incidence and mortality[2]. Europe and Australia, including New Zealand, recorded the highest incidence rate, while Eastern Europe had the highest mortality rates. Projections for 2040 predict a significant rise, with 3.2 million new cases and 1.6 million deaths annually (https://www.who.int).

The CRC primarily affects individuals over the age of 50, with risk factors including diets high in processed meats, low fruit and vegetable intake, sedentary lifestyles, obesity, smoking, and excessive alcohol consumption. Early detection is crucial, as CRC becomes more difficult to treat at advanced stages[3]. Standard treatment options include surgery, targeted therapies, radiotherapy, and chemotherapy; however, drug resistance remains a major obstacle in improving survival rates. New therapeutic strategies, such as small-molecule inhibitors, are being investigated to target the molecular pathways involved in CRC progression and to combat drug resistance effectively[4-6].

Apoptosis signal-regulatory kinase 1 (ASK1) is a key protein in the MAPK family, regulating crucial signaling pathways like JNK and p38, which are activated by cellular stresses such as ROS, ER stress, and inflammation. ASK1 triggers a phosphorylation cascade that affects cellular responses such as apoptosis, inflammation, and proliferation. It also interacts with the Wnt/β-catenin pathway, affecting cancer development by regulating β-catenin stability and promoting its accumulation. Given its central role in stress response and tumorigenesis, ASK1 is a promising target for drug design, especially for phytochemicals aimed at inhibiting cancer progression, including colorectal cancer[7,8].

Phytochemicals have emerged as pivotal components in natural compound-based drug discovery, particularly for cancer chemotherapy, though their impact extends beyond oncology, influencing treatments for a wide range of diseases[9]. Plant-derived small-molecule inhibitors, such as paclitaxel from *Taxus brevifolia* (Pacific yew), and vinblastine and vincristine from *Catharanthus roseus* (Madagascar periwinkle), are cornerstones of modern cancer therapies, targeting cancer cells while minimizing harmful side effects. Beyond cancer, compounds like quinine derived from the bark of *Cinchona* trees revolutionized malaria treatment, while morphine from *Papaver somniferum* (Opium poppy) has been critical in pain management for centuries. Phytochemicals such as resveratrol, found in *Vitis vinifera* (grapevine), and curcumin from *Curcuma longa* (turmeric), have shown promise in addressing cardiovascular diseases, diabetes, and neurodegenerative conditions like Alzheimer's, due to their anti-inflammatory and antioxidant properties[10,11]. The exploration of natural compounds is invaluable, as plant-based drugs often exhibit lower toxicity, fewer side effects, and greater biocompatibility than synthetic drugs. These natural molecules tend to be more selective, targeting specific pathways related to disease progression, which reduces off-target effects and increases treatment efficacy. As resistance to synthetic drugs grows and concerns over their long-term impacts rise, the search for novel phytochemicals offers a safer and more sustainable approach to drug development, paving the way for innovative treatments in various diseases including cancer, infectious diseases, inflammatory conditions, and degenerative disorders[12].

Lannea coromandelica (Houtt.) Merr. (Anacardiaceae) is a deciduous tree, highly valued for its ethnobotanical and medicinal properties. Native to South Asia, including Bangladesh, this tree can grow up to 14 meters tall and is characterized by its alternately arranged pinnate leaves, with five ovate leaflets and branches covered with starry hairs. The unisexual, greenish flowers and ovoid fruits in panicles further distinguish the species taxonomically[13]. *L. coromandelica* has been extensively employed in traditional medicine systems for its therapeutic benefits. The bark, leaves, and resin of this species are well-known for their astringent, antioxidant, anticancer, anti-inflammatory, and antidiabetic properties. Traditionally, this species is used to treat various ailments, including skin disorders such as eczema and psoriasis, digestive issues, and arthritis[14].

To date, no study has been carried out to elucidate the anticancer potential of the *L. coromandelica* phytoconstituents targeting the ASK1 protein. Therefore, we aimed to identify potential small-molecule inhibitors from the bioactive phytochemicals of *L. coromandelica* through a comprehensive structure-based drug design approach targeting the ASK1 receptor, providing insights into a novel treatment strategy for combating CRC.

Materials and Methods

Protein preparation: The ASK1 protein structure, identified by PDB ID "4BHN," was retrieved from the Protein Data Bank, with its structure determined via X-ray diffraction[15]. For receptor preparation, AutoDockTools v.1.5.6 and SWISS-PDB Viewer v.4.10 were utilized. OpenBabel v.3.1.1.1 was then used to convert the energy-minimized protein from PDB to PDBQT format for further analysis[16-18].

Ligand preparation: Phytochemicals from *L. coromandelica* were identified and retrieved from the PubChem and IMPPAT databases in 3D SDF format[19]. Erbitux, known for its efficacy against the ASK1 receptor, was chosen as the control drug and obtained from the PubChem database[20]. All ligands were subjected to energy minimization and subsequently converted to PDBQT format using OpenBabel v.3.1.1.1 for further analysis.

Active site determination: For site-specific molecular docking, the receptor's active site was predicted using the CASTp v.3.0 server[21]. The protein, uploaded in PDB format, was analyzed, and the top-ranked site based on the highest surface area and volume was chosen as the active site for docking simulations.

Molecular docking: A grid box was defined for molecular docking using the output from CASTp v.3.0, with dimensions set to 94 × 64 × 76 and center coordinates of 2.273 × 6.488 × -27.019 along the X, Y, and Z axes, respectively. Molecular docking was performed using EasyDock Vina v.2.237. After docking, the resulting complexes were visualized and analyzed for molecular interactions using BIOVIA Discovery Studio Visualizer[22]. The selected phytocompounds were subsequently subjected to ADMET (absorption, distribution, metabolism, excretion, and toxicity) analysis for further evaluation.

ADMET evaluation: The ADMET evaluation was carried out using the SwissADME server to assess the drug-likeness properties of the compounds[23]. Toxicity parameters were

subsequently assessed through the STopTox server[24]. For both analyses, the compounds were input in SMILES format.

Molecular dynamics simulation: To assess the thermodynamic stability of the control drug and top lead compounds, molecular dynamics (MD) simulations were conducted in a Linux environment using the Desmond module of the Schrödinger 2020-1 package, spanning a duration of 200 ns[25]. The simulated systems were solvated with the SPC water model within orthorhombic periodic boundary boxes, maintaining a minimum distance of 10 Å between the box edges and the solute to uphold constant volume conditions. The OPLS4 force field with default Desmond settings was used for energy minimization of the solvated framework. Simulations were run at a constant temperature of 300 K and a pressure of 1 atm (1.01325 bar) using the NPT ensemble with Nose–Hoover temperature coupling and isotropic pressure scaling. The trajectories were sampled at 200 ps intervals, yielding approximately 1000 frames for subsequent analysis, while the energy data were recorded at 1.2 ps intervals.

Principal component analysis (PCA) and Gibbs free energy landscape (*FEL):* To assess the essential dynamics of the top selected leads and the control drug, PCA was carried out using the Statistics Kingdom server (https://www.statskingdom.com). RMSD and Rg coordinates for all simulated frames were input as two series to complete the PCA calculation using a covariance matrix. For Gibbs FEL analysis, a Python programming script was utilized on Ubuntu Focal Fossa 20.04.6 LTS. The PCA data was initially stored in a CSV file, enabling easy loading and manipulation through the Pandas library. The script leveraged essential libraries such as NumPy for numerical operations, facilitating efficient computation of statistical metrics, and Matplotlib for data visualization. A 2D histogram of the PCA results was generated to estimate the probability distribution of the data points, enabling the calculation of Gibbs free energy based on Boltzmann statistics[26].

MM/GBSA free-energy evaluation: The Prime module of the Schrödinger v.2020-1 package was utilized to compute the MM/GBSA free binding energy. For this calculation, the OPLS4 force field and the VSGB model were applied[10].

Drug target class prediction: The classification of the drug target class was forecasted utilizing the SwissTargetPrediction server. By submitting the canonical SMILES to the server and examining the *Homo sapiens* datasets, the predictions were confirmed[27].

Results and Discussion

Molecular docking study

Seventeen phytochemicals from *L. coromandelica* were successfully docked against the target protein ASK1, revealing a broad spectrum of binding affinities (Fig. 1, Table 1). Among them, arabinose showed the weakest binding affinity with a docking score of -4.4 kcal/mol, while ellagic acid demonstrated the strongest affinity, scoring -9.6 kcal/mol. In comparison, the control drug erbitux yielded a docking score of -7.4 kcal/mol, and notably, 10 of the phytocompounds outperformed the control drug. These top 10 compounds, *i.e.*

ellagic acid, physcion, anthraquinone, morin, quercetin, (+)-leucocyanidin, guaijaverin, leucodelphidin, isoquercitrin, and rutin—underwent for ADMET analysis, which identified two lead candidates: ellagic acid (-9.6 kcal/mol) and physcion (-9.3 kcal/mol). Strong binding affinity is crucial in drug design, as it correlates with a compound's efficacy in inhibiting its target, thereby enhancing its therapeutic potential. A previous study on *Chromolaena odorata* identified seven phytochemicals as ASK1 inhibitors, with binding affinities ranging from -8.14 to -9.10 kcal/mol, with the best candidate odoratin, scoring -9.10 kcal/mol[28]. In comparison, both ellagic acid and physcion from the current study exhibited superior binding affinities, reinforcing their potential as drug candidates.

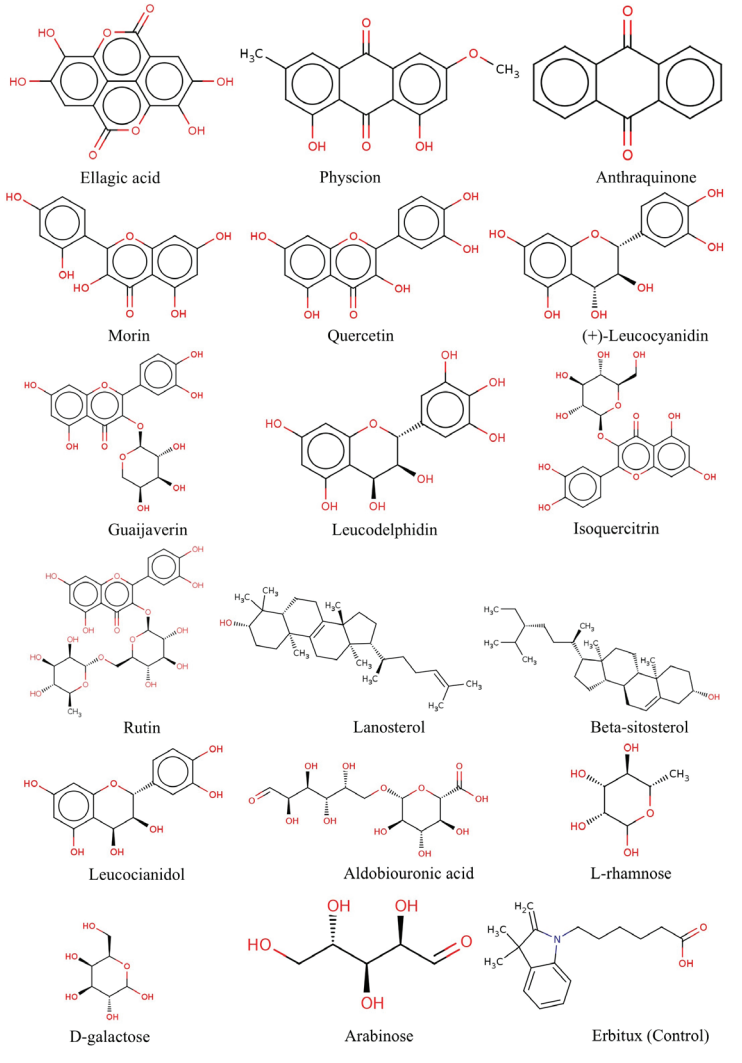

Fig. 1. Chemical structures of the phytocompounds and control drug used in molecular docking analysis.

Table 1. Molecular docking analysis of *Lannea coromandelica* phytocompounds against ASK1 receptor

Sl. No.	Ligands	IMPAAT ID/ PubChem CID	Molecular formula	Molecular weight (g/mol)	Binding affinity (kcal/mol)
1	Ellagic acid	IMPHY005537	$C_{14}H_6O_8$	302.19	-9.6
2	Physcion	IMPHY012117	$C_{16}H_{12}O_5$	284.26	-9.3
3	Anthraquinone	IMPHY007192	$C_{14}H_8O_2$	208.21	-9.0
4	Morin	IMPHY005463	$C_{15}H_{10}O_7$	302.24	-8.9
5	Quercetin	IMPHY004619	$C_{15}H_{10}O_7$	302.24	-8.8
6	(+)-Leucocyanidin	IMPHY011966	$C_{15}H_{14}O_7$	306.27	-8.8
7	Guaijaverin	IMPHY011898	$C_{20}H_{18}O_{11}$	434.35	-8.5
8	Leucodelphidin	IMPHY011885	$C_{15}H_{14}O_8$	322.27	-8.4
9	Isoquercitrin	IMPHY012721	$C_{21}H_{20}O_{12}$	464.38	-8.2
10	Rutin	IMPHY015047	$C_{27}H_{30}O_{16}$	610.52	-8.0
11	Lanosterol	IMPHY011857	$C_{30}H_{50}O$	426.72	-7.2
12	Beta-sitosterol	IMPHY014836	$C_{30}H_{50}O$	414.71	-7.0
13	Leucocianidol	IMPHY011611	$C_{15}H_{14}O_7$	306.27	-6.6
14	Aldobiouronic acid	IMPHY011597	$C_{12}H_{20}O_{12}$	356.28	-6.1
15	L-rhamnose	IMPHY015056	$C_6H_{12}O_5$	164.16	-5.4
16	D-galactose	IMPHY012050	$C_6H_{12}O_6$	180.16	-5.1
17	Arabinose	IMPHY004187	$C_5H_{10}O_5$	150.13	-4.4
18	Erbitux (Control)	85668777	$C_{17}H_{23}NO_2$	273.37	-7.4

Molecular interaction analysis

The two lead compounds, ellagic acid and physcion, along with the control drug erbitux, demonstrated both conventional hydrogen bonding and hydrophobic interactions with key active site residues of the target protein ASK1, which are critical for their inhibitory potential (Fig. 2, Table 2). Binding within the active site is of paramount importance in drug design, as it directly influences the lead compound's ability to modulate the biological functions of the target protein. The active site of a protein contains specific amino acids that are essential for the protein's enzymatic activity or signal transduction processes. When a compound binds tightly within this site, it can effectively block or alter these functions, thereby inhibiting the protein's activity[26].

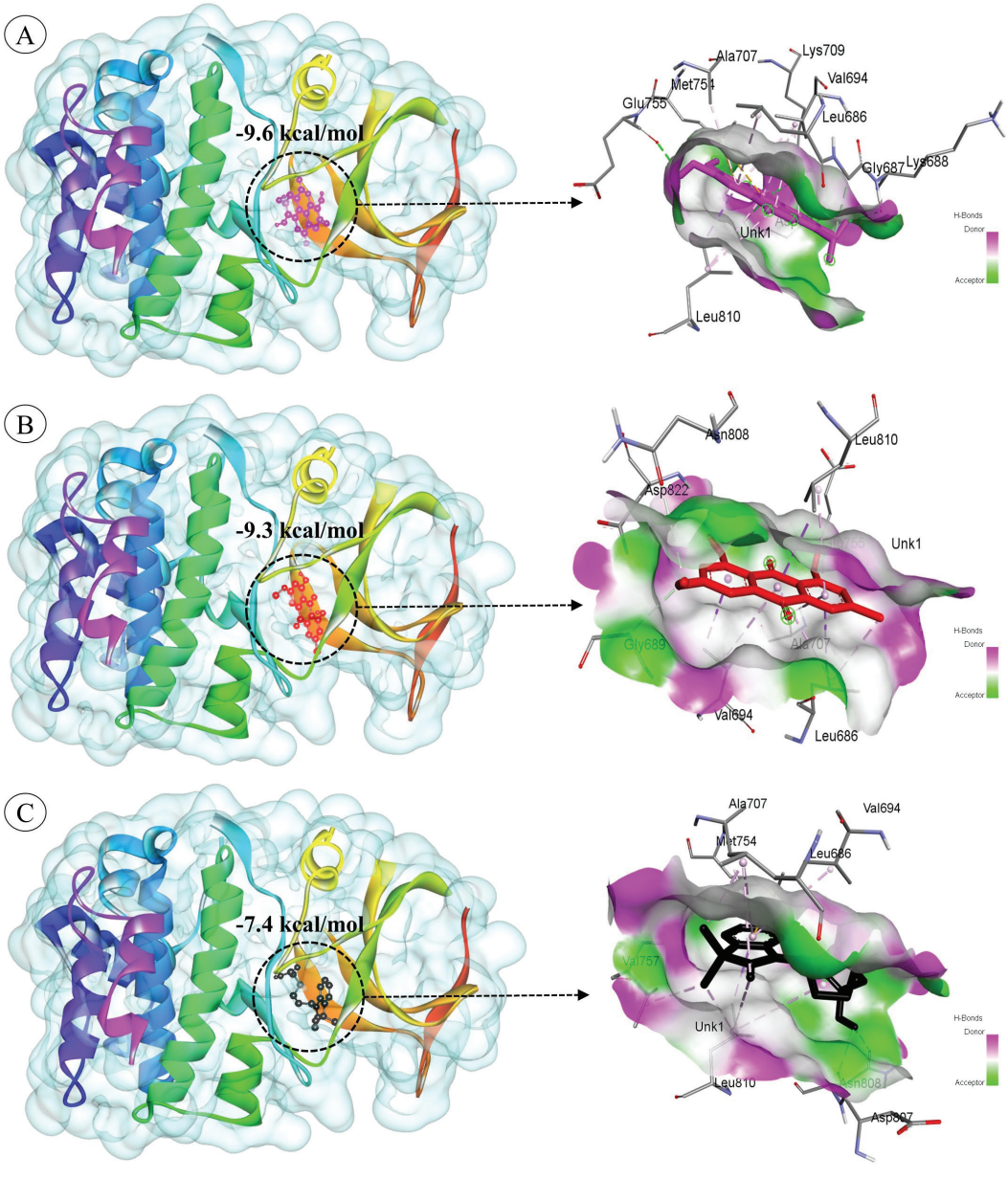

Fig. 2. Site-specific molecular docking analysis illustrating docked complexes and three-dimensional interactions in the binding cavity of ASK1. A. Ellagic acid, B. Physcion, C. Erbitux (control drug).

Table 2. Evaluation of molecular interaction between the lead compounds and the control drug targeting ASK1 protein

Ligands	Binding sites	Hydrogen-bonding residues (Distance in Å)	Number of hydrogen bonds	Hydrophobic-interaction residues	Binding affinity (kcal/mol)
Ellagic acid	Leu686, Gly687, Lys688, Val694, Ala707, Lys709, Met754, Glu755, Leu810, Asp822	Gly688(2.24), Lys709(2.51), Glu755(2.73), Asp822(2.78)	4	Leu686, Gly687, Val694, Ala707, Met754, Leu810	-9.6
Physcion	Leu686, Gly689, Val694, Ala707, Glu755, Asn808, Leu810	Glu755(2.90)	1	Leu686, Gly689, Val694, Ala707, Asn808, Leu810	-9.3
Erbitux (control drug)	Leu686, Val694, Ala707, Met754, Val757, Asp807, Asn808, Leu810	Asp807(2.61), Asn808(2.23)	2	Leu686, Val694, Ala707, Met754, Val757, Leu810	-7.4

Ellagic acid interacted with the residues Leu686, Gly687, Lys688, Val694, Ala707, Lys709, Met754, Glu755, Leu810, and Asp822 (Fig. 3A), forming four conventional hydrogen bonds (CHBs) with Gly688, Lys709, Glu755, and Asp822. In contrast, physcion exhibited interactions with Leu686, Gly689, Val694, Ala707, Glu755, Asn808, and Leu810, forming only one CHB with the Glu755 residue (Fig. 3B). Erbitux interacted with Leu686, Val694, Ala707, Met754, Val757, Asp807, Asn808, and Leu810, with only two residues (Asp807 and Asn808) participating in CHBs (Fig. 3C).

Hydrogen bonding with active site residues increases the specificity and stability of the compound-protein interaction, ensuring that the drug forms a strong and selective bond with ASK1. These interactions help anchor the compound within the binding pocket, enhancing its efficacy by preventing easy dissociation. Additionally, hydrophobic interactions complement hydrogen bonds by further stabilizing the complex. Hydrophobic residues in the active site often form van der Waals interactions with nonpolar regions of the compound, thereby improving the overall binding affinity[28,29].

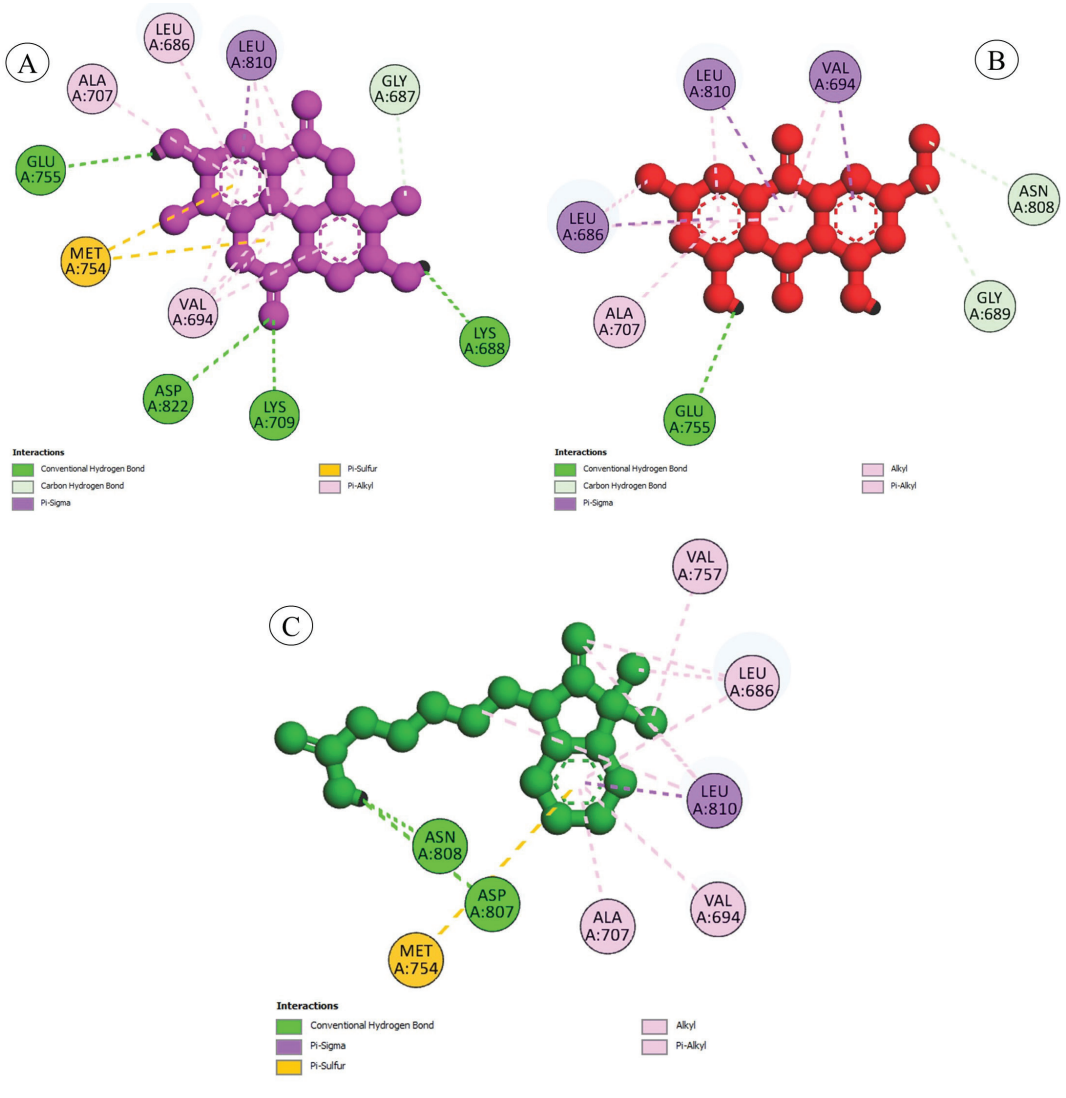

Fig. 3. Molecular interaction analysis in 2D form elucidating hydrogen bonding and hydrophobic interactions. A. Ellagic acid, B. Physcion, C. Erbitux.

ADMET properties evaluation

The ADMET analysis comparing ellagic acid, physcion, and the control drug erbitux revealed similar drug-likeness properties (Table 3, Fig. 4). Both ellagic acid and physcion exhibited stronger binding capabilities with ASK1 due to their higher number of hydrogen bond acceptors and donors, contributing to their robust molecular interactions. Although erbitux displayed slightly higher lipophilicity (3.41), indicating better membrane permeability, the two lead compounds maintained a favorable balance, with ellagic acid

showing a lower consensus log P of 1.00 and Physcion at 2.27 (Table 3). All compounds showed high gastrointestinal absorption; however, erbitux surpassed the leads in blood-brain barrier permeability, which could be advantageous for neurological applications. Regarding drug metabolism, both ellagic acid and physcion shared similar cytochrome enzyme inhibition profiles, particularly for CYP1A2, CYP2C19, and CYP2D6; however, physcion exhibited slight variations in their interactions with CYP3A4 and CYP2C9, which could influence their metabolic clearance[29].

Table 3. ADMET properties evaluation of the lead candidates and Erbitux

Parameters		Compounds		
		Ellagic acid	Physcion	Erbitux (control)
Physicochemical properties	Formula	$C_{14}H_6O_8$	$C_{16}H_{12}O_5$	$C_{17}H_{23}NO_2$
	Molecular weight (g/mol)	302.19	284.26	273.37
	H-bond acceptors	8	5	2
	H-bond donors	4	2	1
	Molar refractivity	75.31	75.25	86.07
	TPSA	141.34 Å^2	83.83 Å^2	40.54 Å^2
Lipophilicity ($logP_{0/w}$)	iLOGP	0.79	2.45	2.74
	XLOGP3	1.10	3.04	3.99
	WLOGP	1.31	2.19	3.56
	MLOGP	0.14	0.61	3.05
	Silicos-IT Log P	1.67	3.07	3.7
	Consensus Log P	1.00	2.27	3.41
Pharmacokinetics	GI absorption	High	High	High
	BBB permeant	No	No	Yes
	Pgp substrate	No	No	No
	CYP1A2	Yes	Yes	Yes
	CYP2C19	No	No	Yes
	CYP2C9	No	Yes	No
	CYP2D6	No	No	No
	CYP3A4	No	Yes	No
	Log Kp	-7.36 cm/s	-5.88 cm/s	-5.13 cm/s
Water solubility (ESOL)	Log S	-2.94	-3.87	-3.87
	Solubility (mg/ml)	3.43E-01	3.80E-02	3.65E-02
	Solubility (mol/l)	1.14E-03	1.34E-04	1.33E-04
	Class	Soluble	Soluble	Soluble
Drug likeness	Lipinski (violations)	0	0	0
	Bioavailability score	0.55	0.55	0.85
Medicinal chemistry	PAINS (alerts)	1 alert	1 alert	0
	Synthetic accessibility	3.17	2.69	2.6

Table 3 Contd.

Parameters		Compounds		
		Ellagic acid	Physcion	Erbitux (control)
Toxicity	Acute inhalation toxicity	Non-toxic	Toxic	Toxic
	Acute oral toxicity	Non-toxic	Non-toxic	Toxic
	Acute dermal toxicity	Toxic	Toxic	Non-toxic
	Eye irritation and corrosion	Toxic	Non-toxic	Non-toxic
	Skin sensitization	Sensitizer	Non-sensitizer	Non-sensitizer
	Skin irritation and corrosion	Negative	Negative	Negative

Water solubility analysis indicated that ellagic acid was the most soluble (-2.94) compared to physcion (-3.87) and erbitux (-3.87) suggesting better oral bioavailability. Despite these variations, all compounds adhered to Lipinski's Rule of Five, with zero violations, reinforcing their drug-likeness[26]. In terms of toxicity, the two lead compounds demonstrated favorable results compared to the control drug erbitux. Although erbitux had a higher bioavailability score (0.85) compared to the lead compounds (0.55), the enhanced safety profile and potent binding affinities of ellagic acid (-9.6 kcal/mol) and physcion (-9.3 kcal/mol) position them as potential drug candidates for further development. The ADMET results of our study are consistent with previous reports[26,28,29].

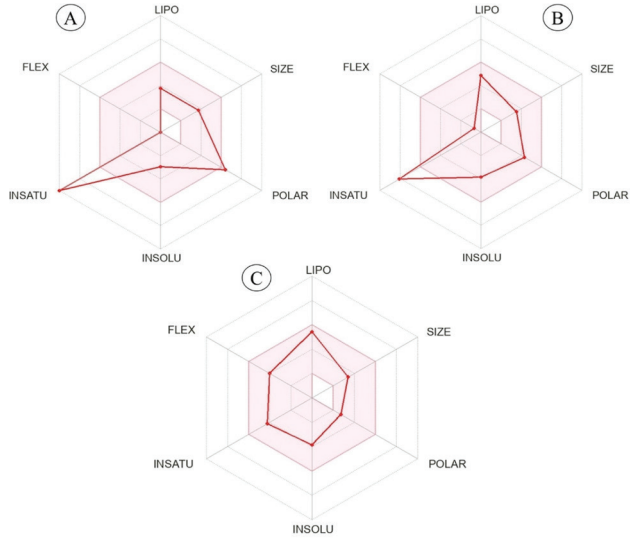

Fig. 4. Drug-likeness and oral bioavailability evaluation of the lead compounds and control drug. LIPO indicates lipophilicity, INSOLU depicts insolubility, INSATU suggests insaturation index, FLEX points flexibility, SIZE implies molecular weight, and POLAR denotes polarity. Pink region reflects the best zone while red line denotes best fit. A. Ellagic acid, B. Physcion, C. Erbitux.

Molecular dynamics simulation

The MD simulation provided key insights into the dynamic behavior of the lead candidates and the control drug, based on a comprehensive 200 ns simulation time frame (Table 4). The C-alpha atom-based protein-ligand (PL) RMSD (root mean square deviation) revealed fluctuations within a very narrow range (< 2.5 Å) for ellagic acid, physcion, and erbitux (Fig. 5A). After 100 ns, ellagic acid and erbitux exhibited similar trajectories until 200 ns simulation, while physcion maintained a steady distance and became more stable from 70 ns onwards. None of the lead compounds or the control drug showed any drastic fluctuations throughout the 200 ns simulation, indicating their significant stability and compactness. The mean PL RMSD value was highest for physcion (1.62 ± 0.24 Å) and lowest for erbitux (1.52 ± 0.12 Å: Table 4).

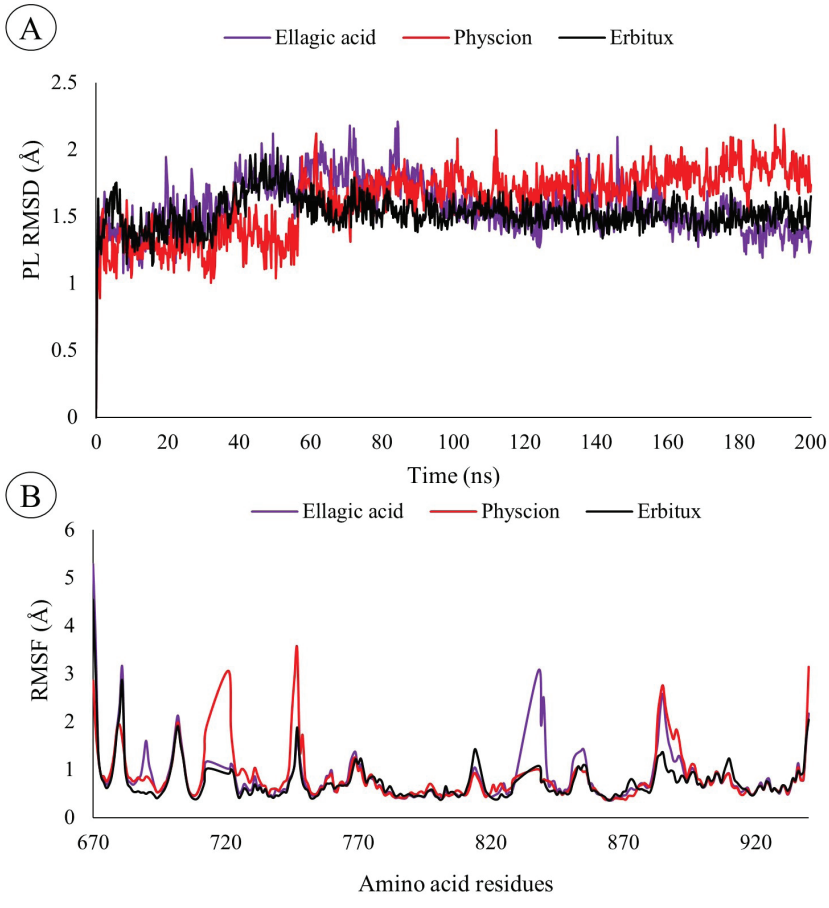

Fig. 5. Molecular dynamics simulation study showing dynamic stability of the tested systems. A. Trajectory based on protein-ligand RMSD, B. Trajectory based on RMSF.

RMSF (root mean square fluctuation) analysis also showcased fluctuations within a narrow range, with the highest mean RMSF observed for physcion (0.85 ± 0.51 Å) and the lowest for erbitux (0.75 ± 0.43 Å). Considering the binding site residues, erbitux had the lowest mean RMSF (0.471 Å), followed by physcion (0.593 Å), and ellagic acid (0.595 Å). Ellagic acid showed the lowest RMSF when interacting with Leu810 (0.469 Å) and the highest RMSF with Lys688 (0.889 Å) (Fig. 5B). Physcion exhibited the lowest RMSF with Leu810 (0.467 Å) and the highest with Gly689 (0.781 Å). Similarly, erbitux depicted the lowest RMSF with Val694 (0.403 Å) and the highest with Val757 (0.593 Å).

Table 4. Molecular dynamics simulation trajectory analysis of the lead compounds and Erbitux

Tested systems	PL RMSD (Å)	RMSF (Å)	Rg (Å)	SASA (Å^2)
Ellagic acid	1.57 ± 0.20	0.83 ± 0.55	3.25 ± 0.01	12.72 ± 9.09
Physcion	1.62 ± 0.24	0.85 ± 0.51	3.47 ± 0.02	98.92 ± 19.81
Erbitux (control)	1.52 ± 0.12	0.75 ± 0.43	3.51 ± 0.07	41.08 ± 9.05

The Rg (radius of gyration) analysis identified ellagic acid as the most stable compound, presenting the lowest mean Rg value (3.25 ± 0.01 Å), followed by physcion (3.47 ± 0.02 Å), and erbitux (3.51 ± 0.07 Å). Ellagic acid maintained remarkable stability throughout the simulation, showing no major fluctuations (Fig. 6A). In contrast, physcion showed slightly higher fluctuations compared to ellagic acid but maintained a steady distance until the end of 200 ns simulation. Erbitux showed some initial movements between 30 to 60 ns (<0.48 Å) and became stable from 60 ns onwards until 200 ns. The Rg profiles demonstrated better compactness for the two lead candidates compared to erbitux, further reinforcing their potential as promising drug candidates.

The SASA (solvent accessible surface area) analysis revealed the lowest mean SASA value for ellagic acid (12.72 ± 9.09 Å^2), followed by erbitux (41.08 ± 9.05 Å^2) and physcion (98.92 ± 19.81 Å^2). In the trajectory graph, ellagic acid maintained its lower position throughout 200 ns, with no major movements (Fig. 6B). Erbitux remained in close proximity to ellagic acid, intersecting at around 110, 120, and 140 ns. Physcion showed some initial fluctuations around 30 to 45 ns, but stabilized from 45 ns onwards until 200 ns, maintaining a steady distance from the other two systems. The SASA profiles further bolstered the similar dynamic behavior of ellagic acid and physcion in relation to the control drug, erbitux. The results of RMSD, RMSF, Rg and SASA from the present investigation align with previously published reports[28].

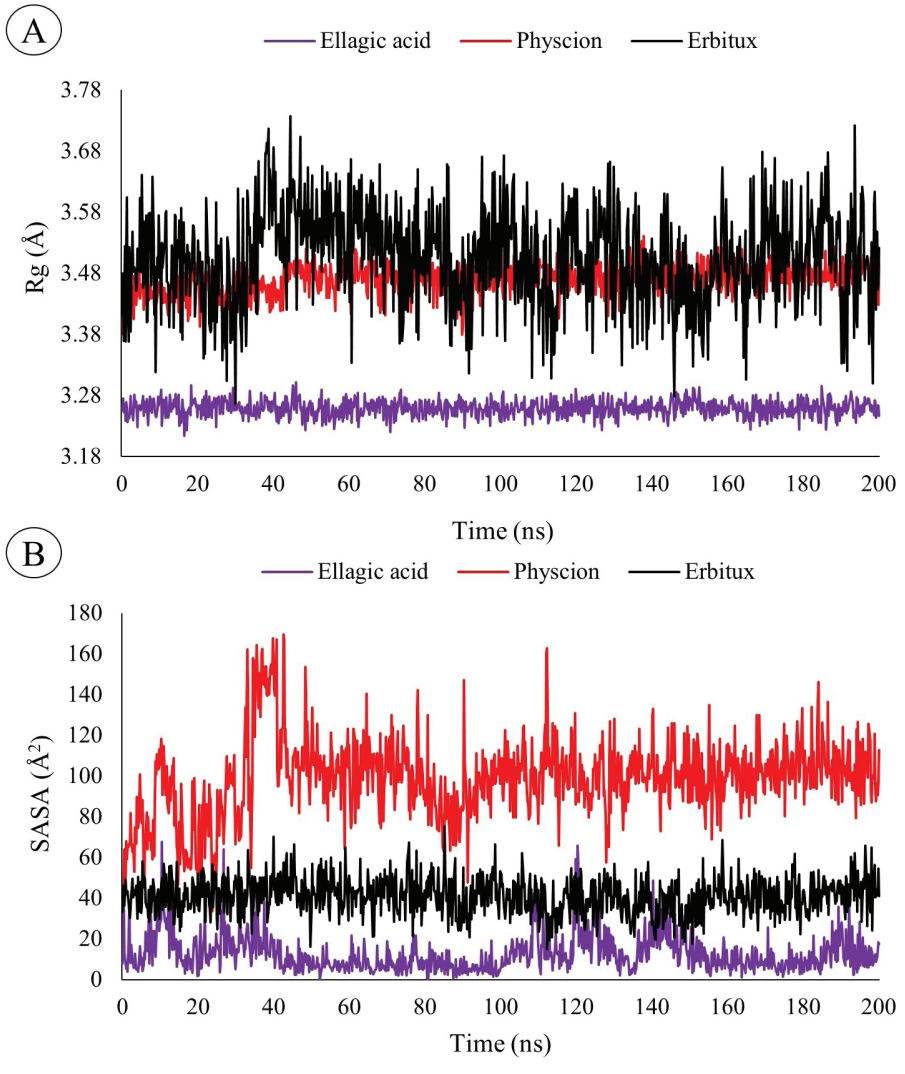

Fig. 6. Molecular dynamics simulation study showing dynamic stability of the tested systems. A. Trajectory based on Rg, B. Trajectory based on SASA.

The protein-ligand contact analysis revealed that both ellagic acid and physcion outperformed erbitux in their interactions with the ASK1 receptor, highlighting their potential as more effective therapeutic candidates (Fig. 7). Ellagic acid formed a diverse array of interactions, including hydrogen bonds, hydrophobic interactions, ionic interactions, and water bridge interactions, contributing to its strong binding affinity. Among these, the Glu755 residue exhibited the highest interaction fraction, underscoring its key role in stabilizing the ligand-receptor complex. Other important residues involved in the interaction were Asp822 and Ser761, with Lys688 and Asp807, contributing brief ionic interactions (Fig. 7A).

In contrast, physcion demonstrated a strong interaction fraction with the Val757 residue, alongside interactions with Leu810 and Gly759. While physcion exhibited a dominant water bridge interaction, it did not form any ionic interactions, indicating a different binding mode from ellagic acid (Fig. 7B). On the contrary, erbitux showed a more limited interaction profile, characterized primarily by hydrogen bonds and hydrophobic interactions. The highest interaction fraction for erbitux was observed with the Ser821 residue, followed by Leu810 and Ala707. Notably, erbitux lacked both ionic and water bridge interactions, which may account for its comparatively lower binding affinity (Fig. 7C).

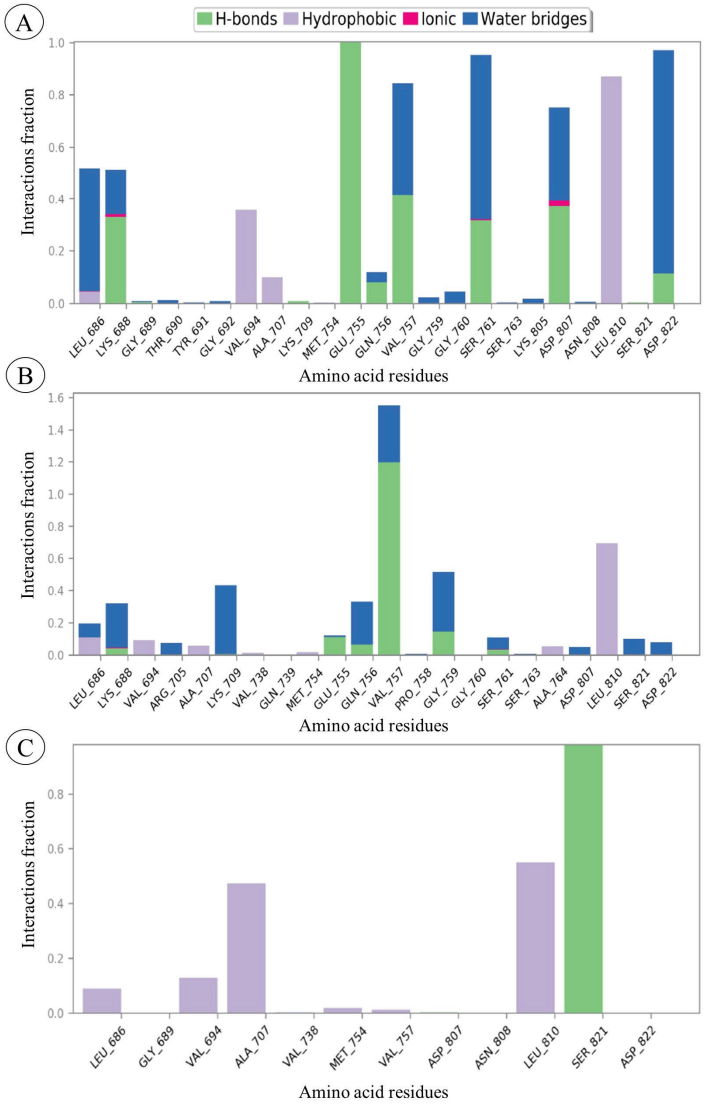

Fig. 7. Evaluation of protein-ligand contacts during molecular dynamics simulation. A. Ellagic acid, B. Physcion, C. Erbitux.

The ligand-torsion profile analysis revealed that Ellagic acid had four rotatable bonds, while physcion had three (Fig. 8).

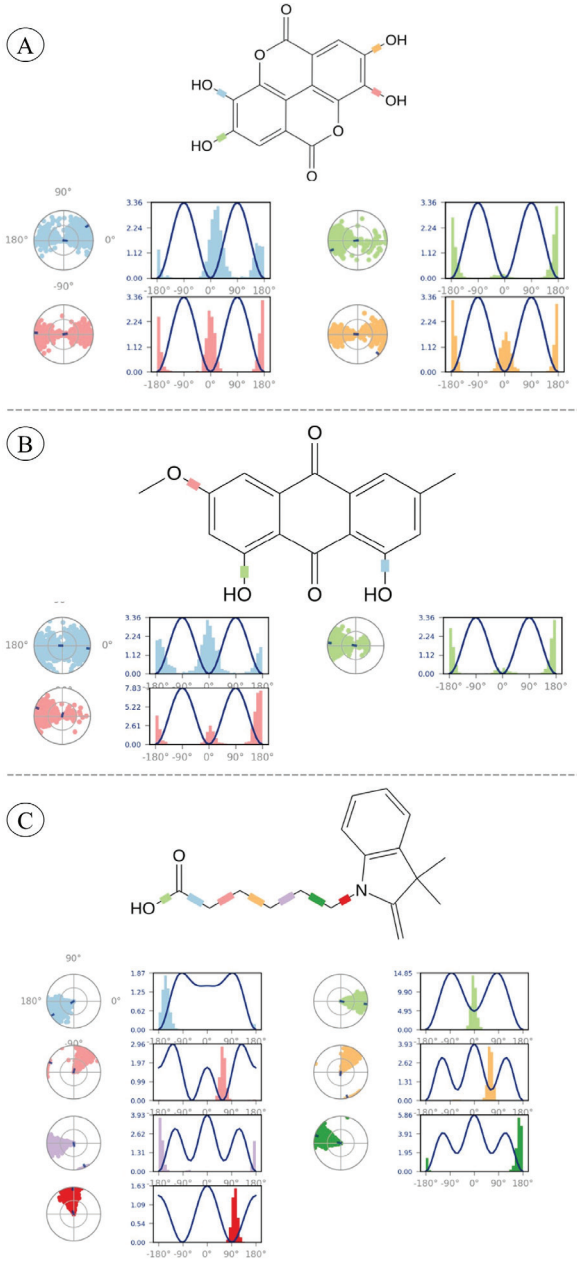

Fig. 8. Evaluation of ligand torsion profiles and rotatable bonds. A. Ellagic acid, B. Physcion, C. Erbitux.

In contrast, the control drug erbitux possessed seven rotatable bonds. This variation in the number of rotatable bonds plays a crucial role in determining the conformational flexibility of the ligands. Fewer rotatable bonds in ellagic acid and physcion suggest a more constrained conformation, which can enhance their binding affinity and specificity for the ASK1 receptor. In contrast, the higher number of rotatable bonds in erbitux indicates greater flexibility, potentially leading to a less stable interaction with the target protein[30]. This finding underscores the potential of ellagic acid and physcion as more effective candidates for targeted therapeutic applications due to their favorable torsional rigidity and resultant binding characteristics.

Principal component analysis (PCA) and Gibbs Free Energy Landscape (FEL)

The PCA and Gibbs FEL analysis provided a comprehensive understanding of the essential dynamics of the two lead compounds and the control drug, erbitux (Fig. 9). In terms of phase-space exploration, ellagic acid demonstrated a broader range, indicating a more flexible dynamic behavior compared to physcion. Conversely, erbitux, despite showing the least phase-space coverage, presented the most stable and favorable results, suggesting more constrained but energetically favorable dynamics. When the phase-space distributions of all three systems were superimposed, highly similar patterns emerged, reflecting comparable global conformational behavior. The Gibbs FEL analysis further supported these findings, showing that erbitux had the most compact and centralized free energy wells (blue areas), indicating lower conformational entropy and greater stability (Fig. 9). Physcion displayed a moderate Gibbs FEL profile with slightly expanded free energy wells, while ellagic acid exhibited the most spread-out energy minima, suggesting a greater diversity of conformational states. This comparative analysis underscored that, despite Erbitux's limited phase-space exploration, its energetic profile was superior, while ellagic acid's broader range suggested increased flexibility but potentially less stable binding dynamics[26].

MM/GBSA free binding energy

The MM/GBSA free binding energy calculations revealed that both ellagic acid and physcion formed more stable complexes with the ASK1 protein compared to the control drug erbitux (Table 5). Specifically, the ellagic acid-protein complex exhibited the most favorable total binding energy (ΔG Bind) of -69.20 kcal/mol, followed by physcion at -65.68 kcal/mol, while erbitux demonstrated a less negative binding energy of -60.75 kcal/mol. Breaking down the energy components, ellagic acid showed significant contributions from coulomb interactions (-21.93 kcal/mol) and lipophilic interactions (-28.03 kcal/mol), despite a slightly unfavorable covalent energy (3.63 kcal/mol). Physcion's complex benefited from moderate coulomb interactions (-9.23 kcal/mol) and substantial lipophilic interactions (-31.48 kcal/mol), along with a nearly neutral covalent energy (-0.13 kcal/mol), indicating stable binding predominantly driven by hydrophobic forces.

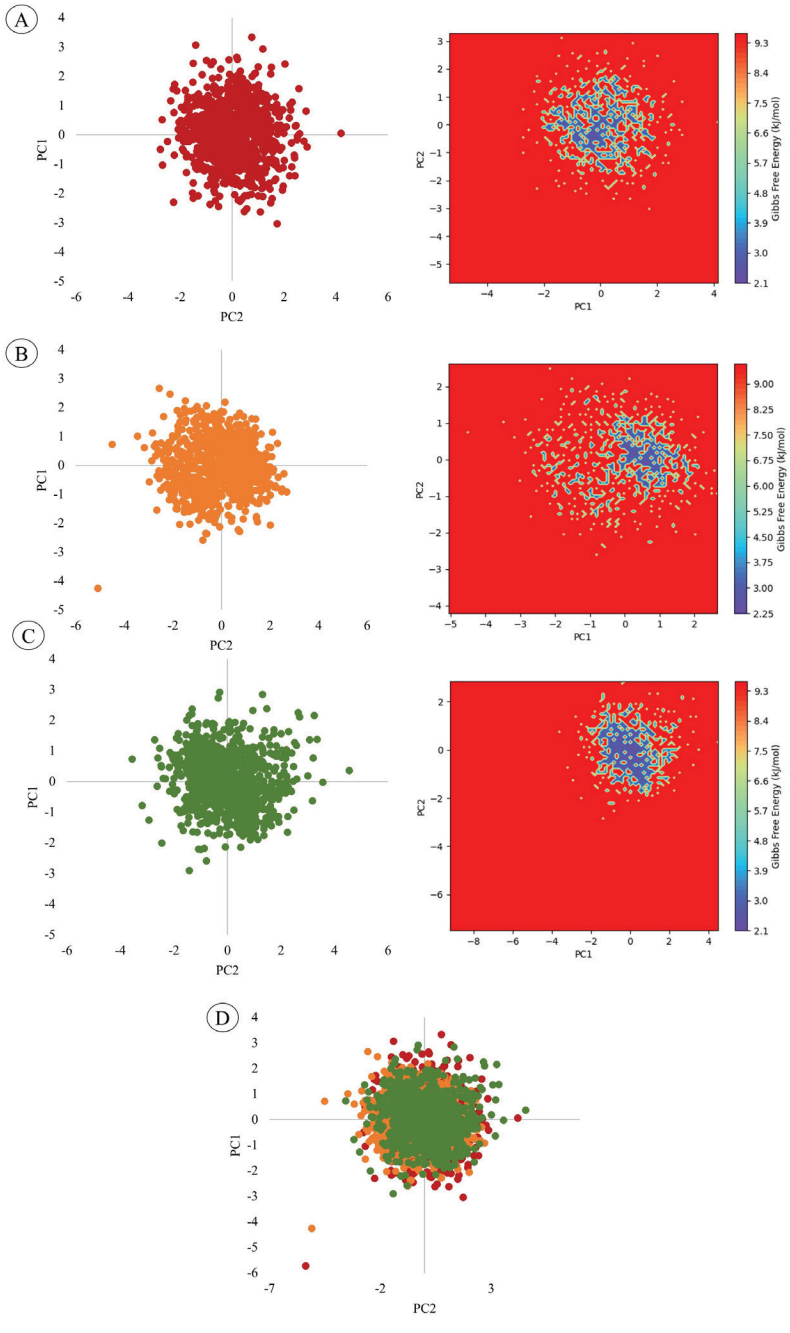

Fig. 9. Evaluation of essential molecular dynamics based on principal components analysis and Gibbs free energy landscapes. A. Ellagic acid, B. Physcion, C. Erbitux, D. Superimposition of two leads and Erbitux.

In contrast, erbitux exhibited a positive coulomb energy (30.33 kcal/mol) and an unfavorable covalent energy (5.04 kcal/mol), although it achieved strong lipophilic interactions (-51.48 kcal/mol) and van der Waals interactions (-34.47 kcal/mol). Additionally, the solvation free energy (ΔG Bind Solv GB) was more favorable for ellagic acid (-41.72 kcal/mol) and physcion (-42.87 kcal/mol) compared to erbitux (-9.20 kcal/mol), further supporting the enhanced binding stability of the lead compounds. These findings underscore the superior binding affinities of ellagic acid and physcion, attributed to their robust electrostatic and hydrophobic interactions, as well as their favorable solvation profiles. Consequently, ellagic acid and physcion emerged as more potent ASK1 inhibitors than erbitux, highlighting their potential as effective therapeutic agents targeting the ASK1 receptor.

Table 5. Free binding energy calculation via MM/GBSA approach

Complexes	Δ G Bind (kcal/mol)	Δ G Coulomb (kcal/mol)	Δ G Covalent (kcal/mol)	Δ G Lipo (kcal/mol)	Δ G Bind Solv GB (kcal/mol)	Δ G Bind vdW (kcal/mol)
Ellagic acid-protein complex	-69.20	-21.93	3.63	-28.03	20.20	-41.72
Physcion-protein complex	-65.68	-9.23	-0.13	-31.48	18.95	-42.87
Erbitux–protein complex (control)	-60.75	30.33	5.04	-51.48	-9.20	-34.47

In a previous study, Omoboyowa et al.[28] conducted an MM/GBSA analysis for the lead compounds derived from *Chromolaena odorata* targeting ASK1, revealing free binding energies ranging from -40.889 to -60.754 kcal/mol, with the control compound scoring -46.235 kcal/mol. In contrast, the present investigation demonstrated significantly improved binding affinities, with free binding energies for our lead compounds spanning from -65.68 to -69.20 kcal/mol, further justifying their candidacy as drug agents.

Drug target class analysis

The drug target class analysis provided valuable insights into the primary biological targets of the lead compounds, further elucidating their potential therapeutic impact. Both ellagic acid and physcion were predominantly associated with kinase as their most frequent target class (Fig. 10). This association is particularly significant, given the crucial role of kinases in cellular signaling pathways, especially in cancer progression and inflammatory diseases. Kinases are involved in regulating cell proliferation, differentiation, and apoptosis, making them prime targets for anticancer therapies.

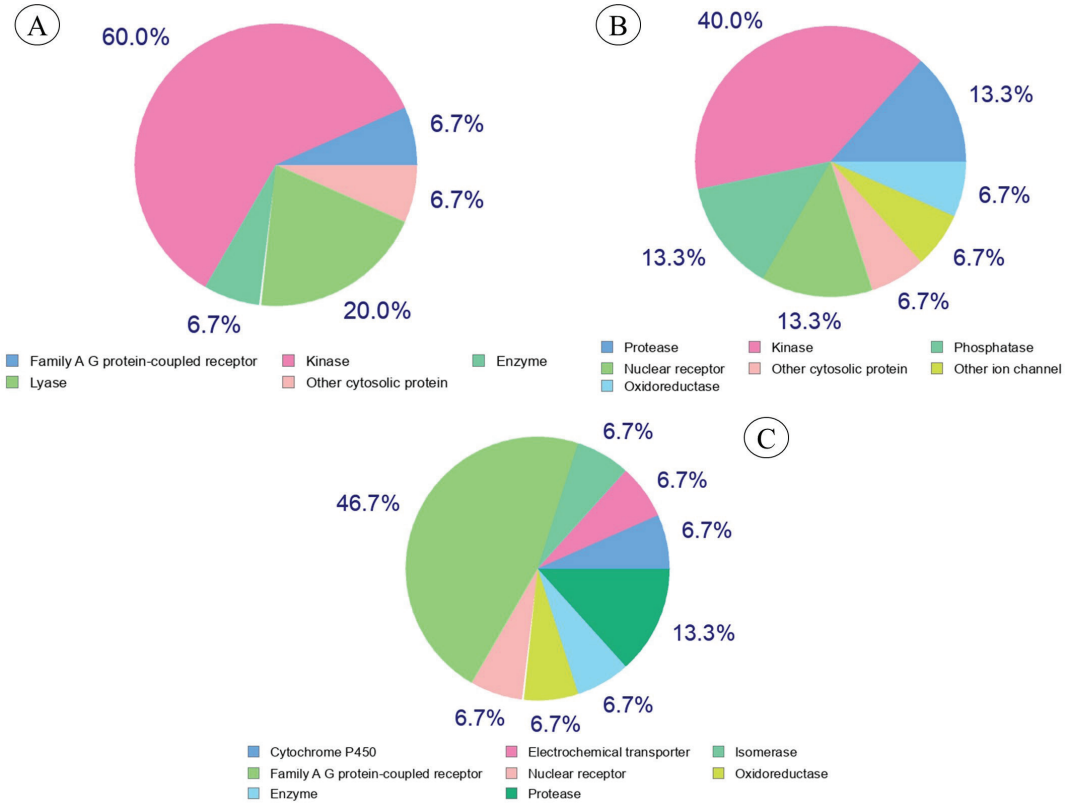

Fig. 10. Drug target class analysis based on *H. sapiens* proteome dataset. A. Ellagic acid, B. Physcion, C. Erbitux.

The identification of kinase as the dominant target class underscores the potential of ellagic acid and physcion to act as effective inhibitors in oncological and inflammatory contexts, aligning with the drug discovery focus on targeting kinase-driven pathways for cancer treatment[31]. In contrast, the control drug erbitux showed a different target profile, with the Family A G protein-coupled receptor (GPCR) emerging as the most dominant target class, followed by proteases. GPCRs play a vital role in mediating a wide array of physiological responses and are among the most exploited drug target classes in therapeutic development[32]. The identification of proteases as a secondary target class suggests that erbitux has a broader mechanism of action, potentially offering efficacy in diverse therapeutic areas beyond kinase inhibition.

Conclusion

In conclusion, our investigation utilized a comprehensive computational biology approach to identify and evaluate potential inhibitors of the ASK1 protein, specifically targeting the inhibition of apoptotic signaling pathways associated with colorectal cancer.

The *in silico* analysis demonstrated that ellagic acid and physcion from *L. coromandelica* possess promising binding affinities and favorable interaction profiles compared to the control drug erbitux. However, it is important to acknowledge several limitations inherent to the computational methods employed. Despite the robustness of molecular docking, molecular dynamics simulations, MM/GBSA, and Gibbs free energy analyses, these methods rely on *in silico* predictions, which may not fully capture the complexities of protein-ligand interactions in biological systems. Consequently, the actual efficacy of ellagic acid and physcion in modulating ASK1 function *in vitro* and *in vivo* remains uncertain, necessitating further experimental validations. Additionally, structure-based drug design faces challenges, such as limited datasets for benchmarking and constrained predictive capabilities, which underscore the importance of complementary wet-lab experiments to substantiate our findings. Nevertheless, despite these challenges, this study offers valuable insights into the potential of *L. coromandelica* as a source of ASK1 inhibitors and lays the foundation for future anticancer drug development efforts targeting colorectal cancer.

Acknowledgement

We gratefully acknowledge the financial support provided by the University of Dhaka, Bangladesh (Reg./ Admin.-3/39297-300), for conducting this study.

References

1. Ranasinghe R, ML Mathai and AA Zulli 2022. Synopsis of modern - day colorectal cancer: Where we stand. Biochim. Biophys. Acta. – Rev. Cancer **1877**:188699.
2. Lopes SR, C Martins, IC Santos, M Teixeira, É Gamito and A Alves 2024. Colorectal cancer screening: A review of current knowledge and progress in research. World J. Gastrointest. Oncol. **16**: 1119-1133.
3. Murphy CC and TA Zaki 2024. Changing epidemiology of colorectal cancer – Birth cohort effects and emerging risk factors. Nat. Rev. Gastroenterol. Hepatol. **21**:25-34.
4. Kusumaningrum AE, S Makaba, E Ali, M Singh, MN Fenjan, I Rasulova, N Misra, SGA Musawi and AA Alsalamy 2024. Perspective on emerging therapies in metastatic colorectal cancer: Focusing on molecular medicine and drug resistance. Cell Biochem. Funct. **42**:e3906.
5. Zheng H, J Liu, Q Cheng, Q Zhang, Y Zhang, L Jiang, Y Huang, W Li, Y Zhao, G Chen, F Yu, L Liu, Y Li, X Liao, L Xu, Y Xiao, Z Zheng, M Li, H Wang, G Hu, L Du and Q Chen 2024. Targeted activation of ferroptosis in colorectal cancer via LGR4 targeting overcomes acquired drug resistance. Nat. Cancer **5**:572-589.
6. Masci D, M Puxeddu, R Silvestri and G La Regina 2024. Metabolic rewiring in cancer: Small molecule inhibitors in colorectal cancer therapy. Molecules **29**:2110.
7. Monastyrskyi A, S Bayle, V Quereda, W Grant, M Cameron, D Duckett and W Roush 2018. Discovery of 2-arylquinazoline derivatives as a new class of ASK1 inhibitors. Bioorg. Med. Chem. Lett. **28**:400-404.
8. Manikanta K, M Paul, VD Sandesha, SS Mahalingam, TN Ramesh, K Harishkumar, SS Koundinya, S Naveen, K Kemparaju and KS Girish 2024. Oxidative stress-induced platelet apoptosis/ activation: Alleviation by purified curcumin via ASK1-JNK/p-38 pathway. Biochem. **89**:417-430.

9. Rahman MO, SS Ahmed, AS Alqahtani, U Cakilcioğlu and MA Akbar 2023. Insight into novel inhibitors from *Sterculia urens* against Cholera via pharmacoinformatics and molecular dynamics simulation approaches. J. Biomol. Struct. Dyn.: 1-22.

10. Ahmed SS, L Suchana, N Sultana and MO Rahman 2023. Unveiling cervical cancer therapeutics from *Abrus precatorius* and *Aphanamixis polystachya*: Insights from molecular docking, dynamics simulation, MM/GBSA and DFT analyses. S. Afr. J. Bot. **163**:561-579.

11. Ahmed MH, SI Karkush, SA Ali and AA Mohammed 2024. Phytochemicals: A new arsenal in drug discovery. Int. J. Med. Sci. Dent. Health **10**(1):29-44.

12. Ashraf MA 2020. Phytochemicals as potential anticancer drugs: Time to ponder nature's bounty. BioMed Res. Int. **2020**(1):8602879.

13. Ahmed ZU, MA Hassan, ZNT Begum, M Khondker, SMH Kabir, M Ahmad, ATA Ahmed, AKA Rahman and EU Haque (Eds) 2009. Encyclopedia of Flora and Fauna of Bangladesh, Vol. **6**. Angiosperm: Dicotyledons (Acanthaceae-Astetaceae). Asiatic Society of Bangladesh, Dhaka, pp. 105-121.

14. Swathi S and K Lakshman 2022. Phytochemistry and pharmacological bio-activities of *Lannea coromandelica*: A review. Innov. J. Med. Sci. **10**(5):1-6.

15. Singh O, A Shillings, PD Craggs, ID Wall, P Rowland, T Skarżyński, CI Hobbs, P Hardwick, R Tanner and M Blunt 2013. Crystal structures of ASK1-inhibtor complexes provide a platform for structure-based drug design. Protein Sci. **22**:1071-1077.

16. El-Hachem N, B Haibe-Kains, A Khalil, FH Kobeissy and G Nemer. *In*: Stevens F, JS Stevens (Eds), AutoDock and AutoDockTools for protein-ligand docking: Beta-site amyloid precursor protein cleaving enzyme 1(BACE1) as a case study. Humana Press, New York, USA, pp. 391-403.

17. Guex N and MC Peitsch 1997. SWISS-MODEL and the Swiss-Pdb Viewer: An environment for comparative protein modeling. Electrophoresis **18**:2714-2723.

18. O'Boyle NM, C Morley and G Hutchison 2008. Pybel: A python wrapper for the OpenBabel cheminformatics toolkit. Chem. Cent. J. **2**:1-7.

19. Vivek-Ananth RP, K Mohanraj, AK Sahoo and A Samal 2023. IMPPAT 2.0: An enhanced and expanded phytochemical atlas of Indian medicinal plants. ACS Omega **8**(9):8827-8845.

20. 20. Ishiguro M, T Watanabe, K Yamaguchi, T Satoh, H Ito, T Seriu, Y Sakata and KA Sugihara 2012. Japanese post-marketing surveillance of Cetuximab (Erbitux®) in patients with metastatic colorectal cancer. Japanese J. Clin. Oncol. **42**:287-294.

21. Tian W, C Chen, L Xue, J Zhao and J Liang 2018. CASTp 3.0: Computed atlas of surface topography of proteins. Nucleic Acids Res. **46**:W363-W367.

22. Minibaeva G, A Ivanová and P Polishchuk 2023. Easydock: Customizable and scalable docking tool. J. Cheminf. **15**:102.

23. Daina A, O Michielin and V Zoete 2017. SwissADME: A free web tool to evaluate pharmacokinetics, drug-likeness and medicinal chemistry friendliness of small molecules. Sci. Rep. **7**:42717.

24. Borba JVVB, VM Alves, RC Braga, D Korn, KE Overdahl, AC Silva, SUS Hall, E Overdahl, N Kleinstreuer, J Strickland, D Allen, CH Andrade, EN Muratov and A Tropsha 2022. Stoptox: An *in silico* alternative to animal testing for acute systemic and topical toxicity. Environ. Health Perspect. **130**:027012.

25. Bergdorf M, A Robinson-Mosher, X Guo, KH Law and DE Shaw 2021. Desmond/GPU performance as of April 2021. DE Shaw Res. Tech. Rep.: 1-7.

26. Ahmed SS and MO Rahman 2024. From flora to pharmaceuticals: 100 new additions to angiosperms of Gafargaon subdistrict in Bangladesh and unraveling antidiabetic drug candidates targeting DPP4 through *in silico* approach. PLoS One **19**(3):e0301348.

27. Daina A, O Michielin and V Zoete 2019. SwissTargetPrediction: Updated data and new features for efficient prediction of protein targets of small molecules. Nucleic Acids Res. **47**:W357-W364.

28. Omoboyowa DA, MN Iqbal, TA Balogun, DS Bodun, JO Fatoki and OE Oyeneyin 2022. Inhibitory potential of phytochemicals from *Chromolaena odorata* L. against apoptosis signal-regulatory kinase 1: A computational model against colorectal cancer. Comput. Toxicol. **23**:100235.

29. Rahman MO and SS Ahmed 2023. Anti-angiogenic potential of bioactive phytochemicals from *Helicteres isora* targeting VEGFR-2 to fight cancer through molecular docking and molecular dynamics simulation. J. Biomol. Struct. Dyn. **41**(15):7447-7462.

30. Hao MH, O Haq and I Muegge 2007. Torsion angle preference and energetics of small-molecule ligands bound to proteins. J. Chem. Inf. Model. **47**(6):2242-2252.

31. Bhullar KS, NO Lagarón, EM McGowan, I Parmar, A Jha, BP Hubbard and HV Rupasinghe 2018. Kinase-targeted cancer therapies: Progress, challenges and future directions. Mol. Cancer **17**:1-20.

32. Hauser AS, MM Attwood, M Rask-Andersen, HB Schiöth and DE Gloriam 2017. Trends in GPCR drug discovery: New agents, targets and indications. Nat. Rev. Drug Discov. **16**(12):829-842.

(Manuscript received on 14 August, 2024; accepted on 18 December, 2024)